

# Coupling $^{18}\text{F}$ -deoxyglucose PET imaging and MRS at 14T of the in vivo GLUT8 knockout mouse brain

C. L. Poityr-Yamate<sup>1</sup>, B. Lanz<sup>1</sup>, H. Lei<sup>1</sup>, F. Prietner<sup>2</sup>, S. Germain<sup>1</sup>, B. Thorens<sup>2</sup>, and R. Gruetter<sup>1,3</sup>

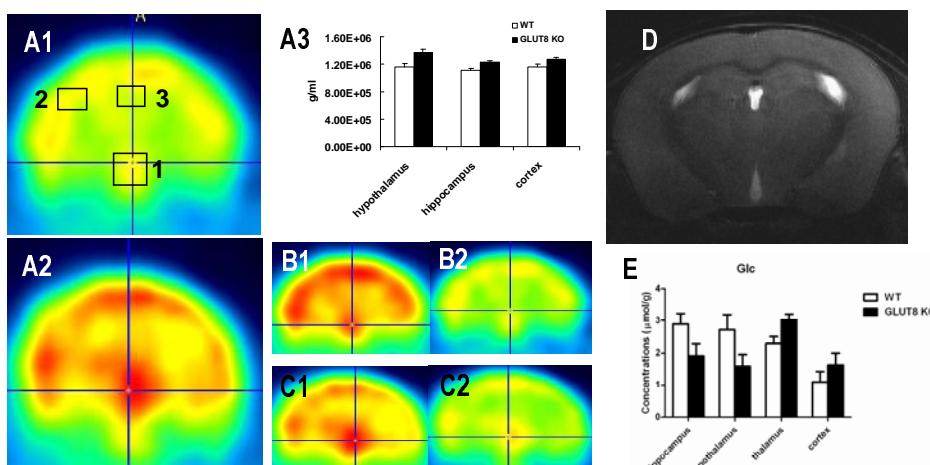
<sup>1</sup>IPMC, EPFL, Lausanne, Vaud, Switzerland, <sup>2</sup>University of Lausanne, Lausanne, Vaud, Switzerland, <sup>3</sup>Radiology, University of Lausanne and Geneva, Switzerland

## Introduction

The physiological function of GLUT8, a recently characterized high-affinity (2mM) glucose transporter expressed in brain, heart, testis and liver (1) still remains uncertain. The goal of this study was to explore whether GLUT8 functions as a glucose transporter under resting physiological conditions using high resolution, in vivo dynamic and steady-state imaging of  $^{18}\text{FDG}$  in brain of GLUT8 knockout (GLUT KO) mice and their wild type (WT) counterparts.

## Methods

Subsequent to magnetic resonance spectroscopic measurements and imaging in a 14.1T/26cm scanner (Varian/Magnex Scientific) mice underwent positron emission tomographic imaging using an avalanche photodiode detector-based LabPET 4 scanner (GammaMedica, Sherbrooke, Canada) achieving a reconstructed volumetric spatial resolution of better than 2.2  $\mu\text{l}$ . For this study we used the glucose analogue 2-[ $^{18}\text{F}$ ]Fluoro-2-deoxy-D-glucose (FDG), a biochemical marker of glucose uptake.  $^{18}\text{FDG}$  dynamic scans (45 min) followed by  $^{18}\text{FDG}$  steady-state scans (60 min) were acquired of the brain after an IV bolus injection (30s) in the femoral vein of  $\sim 50\text{MBq}$ . Storage of coincidence events in list mode files underwent histogramming for image reconstruction (2). Post processing of images was performed using PMOD. GLUT8 KO mice were backcrossed with C57Bl/6 (n=5) and WT (C57Bl/6, n=4) mice (1) were anesthetized with isoflurane (1%, 1 L/min  $\text{O}_2$ ) and vital signs were continuously monitored throughout the scans. Images were semi-quantitated of accumulated intracellular  $^{18}\text{FDG}$ -6-phosphate using standardized uptake values (SUV), expressed as  $[\text{mean ROI activity (kBq/cm}^3)]/[\text{injected dose (kBq)}/\text{body weight (g)}$ . The injected dose per body weight was comparable between WT and GLUT8 KO mice, indicating comparable amounts of  $^{18}\text{FDG}$  entering the systemic blood. Values of SUV therefore allowed comparisons of accumulated intracellular  $^{18}\text{FDG}$ -6-phosphate at steady state between WT and GLUT8 KO mice, as well as comparisons between dynamic (D) and steady-state (st-st) phases of glucose uptake in a given animal. SUV was appropriately color-scaled in the figures, red being maximum.



## Results and Discussion

The distribution and magnitude of phosphorylated  $^{18}\text{FDG}$ , and thereby of glucose uptake in brain at steady-state in GLUT8 KO mice was heterogeneous and *increased* in hypothalamus, cortex and hippocampus (panel A2) relative to WT mice (panel A1). This increase is quantitatively summarized in panel A3.  $^{18}\text{FDG}$  uptake was also modulated in the heart and endocrine organs in GLUT8 KO mice relative to WT mice (results not shown). These observations were unexpected and surprising in light of: (1) the current view that GLUT8 is localized to an intracellular storage site (5); and (2) that regions where modulation of  $^{18}\text{FDG}$  uptake in GLUT8 KO mice was measured correspond to regions where GLUT8 is expressed, e.g. hypothalamus, hippocampus and heart. These differences could not be attributed to excess extracellular  $^{18}\text{FDG}$  judging from washout of non-phosphorylated substrate that occurs during the transition from dynamic to steady-state phases of  $^{18}\text{FDG}$  uptake (panels B and C), nor to differences in glycemia between WT and GLUT8 KO mice (1). Glucose content in hippocampus, hypothalamus and cortex (panel E) was not statistically significant ( $p>0.05$ ) between groups suggesting that normal glucose homeostasis is maintained in the absence of GLUT8. It remains to be explored whether  $^{18}\text{FDG}$  uptake in brain of GLUT8 KO mice may in part reflect up-regulation of other GLUT isoforms or alternatively of glucose transport across intracellular membranes (6).

**Panel A:** full field view at steady-state of  $^{18}\text{FDG}$  PET images in the coronal plane of brain from WT (A1) and GLUT8 KO (A2) mice, located approximately at Bregma position -2.30mm (3). Regions: 1, hypothalamus; 2, cortex; 3, hippocampus; SUV values (A3) by brain region. **Panel B:** Dynamic phase of  $^{18}\text{FDG}$  imaging of WT brain, i.e. substrate uptake and substrate phosphorylation (B1) compared to steady-state phase (B2), i.e. accumulation of phosphorylated substrate and washout of excess  $^{18}\text{FDG}$ . **Panel C:** the same as in Panel B but for GLUT8 KO mouse brain. **Panel D:** T<sub>2</sub>-weighted image corresponding to the Bregma position in panel A. **Panel E:** Localized  $^1\text{H}$  MRS (4) determined levels of glucose (Glc) by brain region in WT (white bar) and GLUT8 KO mice.

**References** (1) Membrez et al., Molecular and Cellular Biology, 2006, 26, 4268-4276; (2) Lecomte et al., IEEE Transactions on Nuclear Science, 2004, 51, 696-704; (3) Paxinos and Franklin, The mouse brain in stereotaxic coordinates, Academic Press 2004; (4) Mlynarik et al., MRM, 2006, 19, 544-553; (5) Widmer et al., Endocrinology, 2005, 146, 4727-4736; (6) Augustin et al., Traffic, 2005, 6, 1196-1212. Supported by the Centre d'Imagerie Biomédicale (CIBM) of the UNIL, UNIGE, CHUV, EPFL and the Leenaards and Jeantet Foundations.